

PACS numbers: 42.55.Px; 42.60.Da; 42.60.Fc
DOI: 10.1070/QE2015v045n12ABEH015855

Double resonance modulation characteristics of optically injection-locked Fabry – Perot lasers

E.S. Dorogush, A.A. Afonenko

Abstract. **The distributed resonator model is used to show the presence of several resonance responses on the modulation characteristic of optically injection-locked Fabry – Perot lasers. The positions of the resonance peaks on the modulation characteristic are determined by the resonator length and frequency detuning of optical injection. It is shown that an appropriate choice of the resonator length and injection locking conditions allows one to obtain efficient modulation in two ranges near 40 – 60 GHz or to increase the direct modulation bandwidth up to 50 GHz.**

Keywords: *optical injection locking, coupled reduced equations, modulation characteristics, modulation bandwidth.*

1. Introduction

The method of optical injection locking of semiconductor lasers is widely used to increase the bandwidth and resonance frequency of direct current modulation [1]. By using strong optical injection locking in experiments with distributed feedback lasers and vertical-cavity surface-emitting lasers, Lau et al. [2] obtained resonance frequency enhancement of 107 and 104 GHz, respectively. The direct modulation bandwidth is in this case limited by a dip of the modulation characteristics and can be increased with increasing pump current of the master laser [3]. For example, in [2] the direct current modulation bandwidth was increased up to 80 GHz in an optically injection-locked vertical-cavity surface-emitting laser. The modulation bandwidth can be also increased by using a system of two or more coupled lasers with different frequency detunings relative to the master laser [4]. In this case, the dip on the modulation characteristic, limiting the modulation bandwidth, is compensated for by additional resonance peaks. Optically injection-locked Fabry – Perot lasers are characterised by the presence of several resonance responses to the modulation characteristic, due to which they can be used for multiple frequency modulation (necessary for multiband communication systems) and to increase the bandwidth of direct current modulation.

The aim of this paper is to study resonances near the unlicensed frequency range of 60 GHz, as well as the possibility of controlling their characteristics. Numerical analysis of modulation processes is based on a system of coupled reduced equations taking into account the longitudinal inhomogeneity of the field and the concentration of charge carriers in the active region.

E.S. Dorogush, A.A. Afonenko Belarusian State University, prosp. Nezavisimosti 4, 220030 Minsk, Republic of Belarus; e-mail: dorogushelena@gmail.com, afonenko@bsu.by

Received 8 May 2015; revision received 16 July 2015
Kvantovaya Elektronika **45** (12) 1121 – 1124 (2015)
Translated by I.A. Ulitkin

2. Distributed resonator model

The field at each point of the active region of the resonator is represented as a combination of forward and backward waves:

$$E(x,t) \propto [A_{\rm m}(x,t)A_0(x){\rm e}^{{\rm i}kx} + B_{\rm m}(x,t)B_0(x){\rm e}^{-{\rm i}kx}]{\rm e}^{-{\rm i}\omega t} + {\rm c.c.} \quad (1)$$

Here, $A_0(x)$, $A_{\rm m}(x, t)$ and $B_0(x)$, $B_{\rm m}(x, t)$ are the stationary and time-varying spatial amplitude components of forward and backward waves; k is the wave propagation constant in a waveguide medium; and ω is the frequency of light in the resonator, which under locking conditions coincides with the frequency of optical injection $\omega_{\rm inj}$.

In the case of optical injection through the right facet of the resonator, the stationary amplitude components satisfy the boundary conditions:

$$A_0(0) = \frac{n_{\rm r}-1}{n_{\rm r}+1}B_0(0), \ \frac{1-n_{\rm r}}{2}A_0(L) + \frac{1+n_r}{2}B_0(L) = B_{\rm inj}, \quad (2)$$

where $n_{\rm r}$ is the refractive index of the active layer; L is the resonator length; and $B_{\rm inj}$ is the injection amplitude.

With field (1), the system of coupled reduced equations for injection-locked Fabry – Perot semiconductor lasers has the form

$$\frac{\partial A_{\rm m}(x,t)}{\partial t} = \frac{v_{\rm g}}{2}(1-{\rm i}\alpha)\Delta G(x,t)A_{\rm m}(x,t) - v_{\rm g}\frac{\partial A_{\rm m}(x,t)}{\partial x},$$
$$\frac{\partial B_{\rm m}(x,t)}{\partial t} = \frac{v_{\rm g}}{2}(1-{\rm i}\alpha)\Delta G(x,t)B_{\rm m}(x,t) + v_{\rm g}\frac{\partial B_{\rm m}(x,t)}{\partial x}. \quad (3)$$

Here, $v_{\rm g}$ is the group velocity of light in the waveguide part of the laser structure; α is the linewidth enhancement factor; $\Delta G(x,t) = G(x,t) - G_0(x)$ is the time-varying component of the mode gain; and $G(x,t)$ and $G_0(x)$ are the mode gains in the dynamic and steady-state regimes, respectively. The gain function has the form:

$$G(x,t) = \frac{gN_0\ln(N(x,t)/N_0)}{1+\varepsilon S(x,t)}, \quad (4)$$

where g is the differential gain; N_0 is the transmission concentration; $N(x, t)$ is the concentration of nonequilibrium charge carriers; ε is the nonlinear gain; and

$$S(x,t) = |A_0(x)|^2 |A_{\rm m}(x,t)|^2 + |B_0(x)|^2 |B_m(x,t)|^2 \quad (5)$$

is the density of photons in the resonator.

The distribution of the charge carrier concentration N is found from the equation

$$\frac{dN(x,t)}{dt} = \frac{j(t)}{e} - R(x,t) - R_{\rm st}(x,t), \quad (6)$$

where $j(t)$ is the density of the pump current; $R(x,t) = N(x,t)/\tau$ and $R_{\rm st}(x,t) = v_{\rm g}G(x,t)S(x,t)$ are the rates of spontaneous and stimulated recombination of nonequilibrium charge carriers, respectively; τ is the lifetime of nonequilibrium charge carriers; and e is the electron charge.

Consider the case of the injection modulation by the pump current at frequency Ω:

$$j(t) = j_0 + j_{\rm m}{\rm e}^{{\rm i}\Omega t} + j_{\rm m}^*{\rm e}^{-{\rm i}\Omega t}, \quad (7)$$

where j_0 and $j_{\rm m}$ are the constant and modulation components of the pump current density. For the modulation characteristics to be obtained in the small-signal regime, the time-varying components of the fields can be conveniently represented as

$$A_{\rm m}(x,t) = 1 + A_{\rm m1}(x){\rm e}^{{\rm i}\Omega t} + A_{\rm m2}^*(x){\rm e}^{-{\rm i}\Omega t},$$
$$B_{\rm m}(x,t) = 1 + B_{\rm m1}(x){\rm e}^{{\rm i}\Omega t} + B_{\rm m2}^*(x){\rm e}^{-{\rm i}\Omega t}, \quad (8)$$
$$\Delta G(x,t) = G_{\rm m}(x){\rm e}^{{\rm i}\Omega t} + G_{\rm m}^*(x){\rm e}^{-{\rm i}\Omega t}.$$

Then the system of coupled reduced equations (3) takes the form

$$\frac{\partial A_{\rm m1}(x)}{\partial x} = \frac{1}{2}(1-{\rm i}\alpha)G_{\rm m}(x) - \frac{{\rm i}\Omega}{v_{\rm g}}A_{\rm m1}(x),$$
$$\frac{\partial B_{\rm m1}(x)}{\partial x} = -\frac{1}{2}(1-{\rm i}\alpha)G_{\rm m}(x) - \frac{{\rm i}\Omega}{v_{\rm g}}B_{\rm m1}(x),$$
$$\frac{\partial A_{\rm m2}(x)}{\partial x} = \frac{1}{2}(1+{\rm i}\alpha)G_{\rm m}(x) - \frac{{\rm i}\Omega}{v_{\rm g}}A_{\rm m2}(x), \quad (9)$$
$$\frac{\partial B_{\rm m2}(x)}{\partial x} = -\frac{1}{2}(1+{\rm i}\alpha)G_{\rm m}(x) + \frac{{\rm i}\Omega}{v_{\rm g}}B_{\rm m2}(x).$$

The value of $G_{\rm m}$ is expressed implicitly from the balance equation of nonequilibrium charge carriers (6):

$$G_m(x) = \left\{\frac{j_{\rm m}}{e}\frac{\partial G(x)}{\partial N(x)} + \left[\left({\rm i}\Omega + \frac{\partial R(x)}{\partial N(x)}\right)\frac{\partial G(x)}{\partial S(x)} - v_{\rm g}G_0(x)\frac{\partial G(x)}{\partial N(x)}\right]S_{\rm m}(x)\right\}$$
$$\times\left[{\rm i}\Omega + \frac{\partial R(x)}{\partial N(x)} + v_{\rm g}\frac{\partial G(x)}{\partial N(x)}S_0(x)\right]^{-1}, \quad (10)$$

where

$$S_{\rm m}(x) = |A_0(x)|^2[A_{\rm m1}(x) + A_{\rm m2}(x)] + |B_0(x)|^2[B_{\rm m1}(x) + B_{\rm m2}(x)] \quad (11)$$

is the modulation component of the photon density in the resonator.

In this case, the variables of the field components satisfy the boundary conditions:

$$A_{\rm m1}(0) = B_{\rm m1}(0),\ B_0(L)B_{\rm m1}(L) = \frac{n_{\rm r}-1}{n_{\rm r}+1}A_0(L)A_{\rm m1}(L),$$
$$A_{\rm m2}(0) = B_{\rm m2}(0),\ B_0^*(L)B_{\rm m2}(L) = \frac{n_{\rm r}-1}{n_{\rm r}+1}A_0^*(L)A_{\rm m2}(L). \quad (12)$$

3. Resonance modulation bandwidth

The optically injection-locked laser operates below the threshold, amplifying the injection light at frequency $\omega_{\rm inj}$. In contrast to a travelling-wave amplifier [5], of fundamental importance for the generation dynamics is the presence of eigenmodes of an optical resonator. In the case of harmonic amplitude modulation of the current with frequency Ω, the spectrum of the laser on either side of the carrier frequency exhibits two side frequencies detuned from the carrier one by $\pm\Omega$. When the side frequency coincides with the frequency of the resonator eigenmode (shifted to lower frequencies compared to the free-running regime), there is a resonance increase in the amplitude of the side modes [6]. A specific feature of the Fabry–Perot resonator is a set of equivalent modes, spaced from each other by the frequency $\omega_{\rm m} = 2\pi v_{\rm g}/2L$; therefore, in lasers with this type of resonator one should observe a set of periodically spaced resonant responses on the modulation characteristic – at each coincidence of the side frequency with one of the resonator eigenfrequencies.

Figure 1 shows the calculated modulation components of the output power, normalised to the value of the effectiveness of low-frequency modulation dP_0/dI in the free-running regime (relative modulation efficiency), at different detunings of injection frequencies of lasers with resonator lengths of 260 and 390 μm. The laser parameters used in the numerical experiment are given below. The value of dP_0/dI at the chosen laser parameters slightly (within 0.33–0.35 W A^{-1}) depended on the resonator length.

Slave laser wavelength λ/μm	1.55
Laser diode resonator width W/μm	2.5
Resonator phase refractive index $n_{\rm r}$	3.3
Resonator group refractive index $n_{\rm g}$	3.8
Effective lifetime of charge carriers τ/ns	1
Differential gain g/cm	5×10^{-11}
Transparency carrier concentration N_0/cm^{-2}	5×10^{11}
Nonlinear gain ε/cm^2	10^{-12}
Linewidth enhancement factor α	3
Internal loss coefficient ρ/cm^{-1}	5

At injection current modulation frequencies, multiple of the intermode interval of the resonator, the amplitude of the modulation component of the laser output from the side of the resonator facet through which optical injection is per-

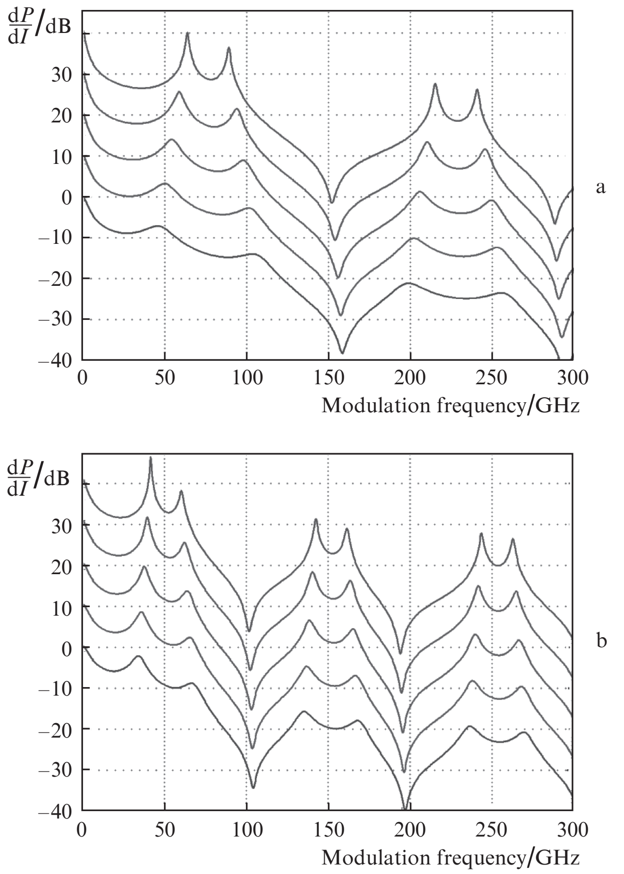

Figure 1. Behaviour of the relative modulation efficiency of a laser with a resonator length of (a) 260 and (b) 390 μm with increasing detuning within the locking band; the injection power is 15 mW, the pump current is 25 mA, the efficiency of low-frequency modulation in the free-running regime is $dP_0/dI \approx 0.35$ W A^{-1}, and the step of upward displacement of the curves at different detunings is 10 dB.

formed vanishes (for the output from the opposite facet such dips are observed when the modulation frequency is multiple of the doubled intermode interval). Such a reduction in the generation efficiency of a modulated wave is related to its 2π-fold phase shift with respect to the induced field sources during a resonator round-trip, which is not compensated for, as is the case of the free-running regime, by an unlimited increase in the Q-modulated mode when approaching its frequency to the frequency of the resonator eigenmode.

Calculations have shown the presence of periodic high-frequency resonance responses on the modulation curves. The intensity of the resonance increases by changing the detuning of the injection frequency from negative to positive values within the locking band, because at negative frequency detunings the gain in the active region of the resonator is substantially below the threshold, and the resonator eigenmodes are strongly suppressed, i.e. their decay time (inversely proportional to the resonance width) is small.

By changing the frequency detuning to a positive value the gain is increased, approaching the threshold one [7], and the decay time of eigenmodes increases. The maximum value of modulation responses will be achieved at the boundary of the locking region, where the gain is equal to the lasing threshold. In the region adjacent to this boundary, the regime of injection locking can be unstable, i.e. the laser will generate self-sustained oscillations. Near the lasing threshold when the change in resonator eigenfrequencies can be neglected, the resonance responses will be observed at modulation frequencies

$$\Omega_{res} = \kappa\Delta\omega_m \pm \Delta\omega_{inj}, \quad \kappa = 0, 1, 2.... \qquad (13)$$

Of practical interest in this case are the first two maximal responses. The frequency of the first resonance, as in the case of single-mode lasers, is determined by the frequency detuning of external injection. The frequency of the second resonance on the modulation characteristic depends on the intermode interval of the resonator at a given frequency detuning. Thus, by selecting the resonator length, one can achieve efficient modulation at two frequencies corresponding to the first two resonance response on the modulation characteristic. Thus, when the resonator length is $L = 260$ μm (Fig. 1a), resonance peaks are observed at 60 and 90 GHz, and at $L = 390$ μm (Fig. 1b) – at 40 and 60 GHz.

4. Increase in the direct modulation bandwidth

While simultaneously increasing the injection power and the pump current at which the locking bandwidth is preserved, the depth of dips of the modulation curves between resonance peaks decreases (Fig. 2). Thus, with increasing pump current from 20 to 50 mA (I_{th} = 3.5 mA) and at a corresponding increase in injection power from 12 to 32 mW, the modulation efficiency in the dips changed from 0.06 W A^{-1} (–8 dB) to 0.2 W A^{-1} (–2.4 dB).

As can be seen from Fig. 2, the direct modulation bandwidth (frequency range in which the modulation efficiency is reduced by 3 dB relative to the low frequency value) is limited by the first dip of the modulation characteristic. With a further increase in the pump current and injection power, the depth of the dip is reduced. If the depth of the dip is reduced to a level of – 3 dB, the direct modulation bandwidth will significantly increase due to the addition of resonance regions (Fig. 3). Since the maximum injection current is limited, the dip before the first resonance can also be reduced due to lower frequency detunings of external injection. In this case, the

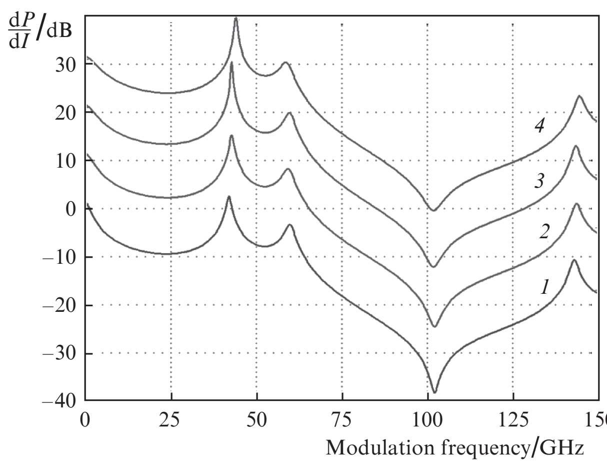

Figure 2. Behaviour of the relative modulation efficiency of a laser with a resonator length $L = 390$ μm with increasing simultaneously the pump current and injection power: (*1*) I = 20 mA and P_{inj} = 12 mW, (*2*) 30 mA and 19 mW, (*3*) 40 mA and 25 mW, and (*4*) 50 mA and 32 mW; $dP_0/dI \approx 0.35$ W A^{-1}, and the step of upward displacement of the curves at different detunings is 10 dB.

first response is shifted to the left on the modulation curve, reducing the dip and the second resonance, according to (13), moves to the right, increasing the depth of the dip between the first two resonances. In lasers with longer resonators, i.e. with a smaller intermode interval, the width of the dips on the modulation characteristic is less; therefore, one can easily increase the direct modulation bandwidth in these lasers than in lasers with a short resonator. Figure 3 shows the modulation characteristics of the four lasers with different resonator lengths. The pump current in all the cases was the same and equal to 80 mA.

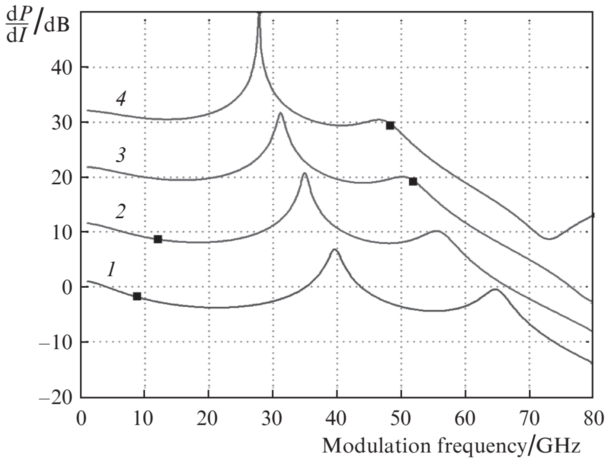

Figure 3. Behaviour of the relative modulation efficiency of a laser with a resonator length of (*1*) 390, (*2*) 450, (*3*) 500 and (*4*) 550 μm; squares shows the boundaries of the direct modulation bandwidth at a level of –3 dB, $dP_0/dI \approx$ 0.34 W A^{-1}, and the step of upward displacement of the curves at different detunings is 10 dB.

The values of the frequency detuning and the external injection power were chosen from the condition of a simultaneous decrease in the first two dips of the modulation characteristic. At resonator lengths of 390, 450, 500 and 550 μm, the direct modulation bandwidths were 9, 12, 52 and 48 GHz, respectively. A further increase in the resonator length will not lead to a broadening of the modulation bandwidth in excess of that achieved due to the reduction of the intermode interval.

It should be noted that in the selected model we did not take into account the transfer processes of charge carriers in the active region and capture in quantum wells [8]. These processes reduce the modulation efficiency at high frequencies, but do not fundamentally affect the proposed method of increasing the direct modulation bandwidth.

5. Conclusions

We have studied multi-resonance modulation characteristics of optically injection-locked Fabry–Perot semiconductor lasers. Using a system of coupled reduced equations we have developed a model of a distributed resonator. It is shown that the multi-resonance behaviour of the modulation characteristic of these lasers is determined by the presence of equivalent and equidistant resonator modes, whereas the position of the resonance on the frequency axis is governed by the value of the intermode interval of the resonator and the detuning frequency of the master laser. Thus, for lasers with a resonator length of 250–500 μm, the first two maximal responses of the modulation characteristic lie in the range of 40–90 GHz.

We have proposed a method for increasing the direct modulation bandwidth by optimising the position of the second resonance (i.e., by choosing the resonator length, pump current, master laser power and frequency). For example, for a laser with a resonator length of 500 μm at a pump current of 80 mA and an injection power of 40 mW the calculated modulation bandwidth is 50 GHz.

References

1. Qi X.-Q., Liu J.-M. *IEEE J. Sel. Top. Quantum Electron.*, **17** (5), 1198 (2011).
2. Lau E.K., Zhao X., Sung H.-K., Parekh D., Chang-Hasnain C., Wu M.C. *Opt. Express*, **16** (9), 6609 (2008).
3. Lau E.K., Sung H.-K., Wu M.C. *IEEE J. Quantum Electron.*, **44** (1), 90 (2008).
4. Zhao X., Parekh D., Lau E.K, Sung H.-K., Wu M.C., Hofmann W., Amann M.C., Chang-Hasnain C.J. *Opt. Express*, **15** (22), 14810 (2007).
5. Bogatov A.P., Drakin A.E., D'yachkov N.V. *Kvantovaya Elektronika*, **40** (9), 782 (2010) [*Quantum Electron.*, **40** (9), 782 (2010)].
6. Chang-Hasnain C.J., Zhao X. *Optical Fiber Telecommunications V A: Components and Subsystems* (San Diego: Acad. Press, 2008) p. 145.
7. Henry C.H., Olsson N.A., Dutta N.K. *IEEE J. Quantum Electron.*, **21** (8), 1152 (1985).
8. Ushakov D.V., Afonenko A.A., Aleshkin V.Ya. *Kvantovaya Elektronika*, **43** (11), 999 (2013) [*Quantum Electronics*, **43** (11), 999 (2013)].